

Higher calcification costs at lower temperatures do not break the temperature-size rule in an intertidal gastropod with determinate growth

Takahiro Irie · Naoko Morimoto · Klaus Fischer

Received: 30 October 2012 / Accepted: 2 May 2013 / Published online: 16 May 2013
© Springer-Verlag Berlin Heidelberg 2013

Abstract The vast majority of ectothermic organisms grow larger when developing at cooler environmental temperatures, a pattern frequently referred to as the temperature-size rule (TSR). Assuming that this reaction norm has adaptive significance, life history theory predicts that converse patterns may evolve if favored by natural selection, namely if the costs associated with complying to the TSR outweigh the benefits. Calcifying ectotherms may comprise such an exception not following the TSR, because calcification is expected to be more costly at lower temperatures thus increasing associated costs. To test this hypothesis, we reared wild-caught juveniles of the intertidal gastropod *Monetaria annulus* and compared their shell sizes at the end of the juvenile stage between two rearing temperatures. Contrary to our prediction, *M. annulus* does follow the TSR, suggesting that increased calcification costs at lower temperatures are not high enough to break the TSR. Such plastic responses should be considered when interpreting geographical patterns such as latitudinal size clines, which may be caused at least partly by phenotypic plasticity.

Introduction

Most ectotherms mature at a larger size at lower developmental temperatures, a pattern of wide taxonomic prevalence which has been coined the temperature-size rule (TSR; Atkinson 1994). The TSR may comprise either a non-adaptive physiological interaction of an organism with its environment (van Voorhies 1996; van der Have and de Jong 1996; Zuo et al. 2012) or may have adaptive significance (Partridge and French 1996; Angilletta and Dunham 2003; Walters and Hassall 2006). Seeking for a general explanation applicable to all ectothermic taxa, Angilletta et al. (2004) have reviewed several hypotheses based on, for example, the compound interest hypothesis (Partridge and French 1996; Fischer and Fiedler 2002; Atkinson et al. 2003), differential thermal sensitivities of anabolic and catabolic processes (Angilletta and Dunham 2003; Kozłowski et al. 2004), and a positive correlation between temperature and juvenile mortality (Atkinson 1994, 1995, 1996; Irie and Iwasa 2003). Arendt (2010) demonstrated that the TSR may evolve if fecundity increases more steeply with adult body size in cold than in warm environments. Despite these research efforts, the TSR has remained enigmatic and a general explanation for its widespread occurrence is still lacking.

In order to distinguish between the existing hypotheses outlined above, the study of systems comprising exceptions to the TSR along with the respective species' ecology should prove particularly valuable. Atkinson (1995), for instance, mentioned six exceptions to the TSR, one marine diatom, one parasitic copepod, and four mayfly species (see also Walters and Hassall 2006; Zuo et al. 2012). Although the suspected causal factors differed among species, all explanations followed the same straight forward logic: ectotherms follow the TSR if the benefits of complying

Communicated by P. Kraufvelin.

T. Irie (✉)
Department of Biology, Stanford University, Stanford, CA
94305, USA
e-mail: irie@bio-math10.biology.kyushu-u.ac.jp

N. Morimoto
Atmosphere and Ocean Research Institute, The University of
Tokyo, 5-1-5 Kashiwanoha, Kashiwa-shi, Chiba 277-8564,
Japan

K. Fischer
Zoological Institute and Museum, University of Greifswald,
Johann-Sebastian-Bach-Str. 11/12, 17489 Greifswald, Germany

with it outweigh the costs, and exceptions occur in case some “additional costs” invert the balance of fitness. The general benefits and costs of following the TSR might be similar across taxa (Angilletta et al. 2004), while any additional or extraordinary costs may stem from the species-specific ecological background.

Some of the above hypotheses can be tested with optimality models, in which the optimal maturation size at a given temperature is determined by the balance between the benefits of enlarging adult size (referred to as adult size advantage, abbreviated as ASA) and the fitness loss of extending the growth period (the delayed maturation disadvantage, DMD). According to such models, the TSR is evolutionarily maintained, if the optimal maturation size is smaller at higher temperatures (e.g., Kingsolver and Huey 2008). This can be achieved if, for example, the fitness increment of early maturation is larger at higher temperatures (Fig. 1a). More specifically, a positive correlation between temperature and juvenile mortality should select for the TSR, because earlier maturation at higher temperatures mitigates the fitness loss of increased mortality (Atkinson 1994, 1995, 1996; Irie and Iwasa 2003). Moreover, a shorter generation time will increase population growth rate and thereby involves compound interest benefits (Partridge and French 1996; Fischer and Fiedler 2002; Atkinson et al. 2003). However, these effects can be cancelled out, if (1) growth rates decrease very steeply with decreasing temperature and/or if (2) growth rates are simply very slow (see “Appendix 1”). As a result, natural selection may favor thermal reaction norms opposite to the TSR (Fig. 1b). In this case, the very slow growth due to low temperatures can be regarded as the additional cost mentioned above.

One example for such an additional cost which may result in not following the TSR may be calcification, that is, the construction of an exoskeleton in marine ectotherms. We assume two reasons that calcification at low temperatures results in very low growth rates thus selecting against the TSR. First, as the solubility of calcium carbonate (CaCO_3) increases with decreasing temperature, calcification is expected to be more costly at lower temperatures (Vermeij 1987; Morse et al. 2007). Accumulating evidence suggests this relationship holds regardless of whether seawater is undersaturated with CaCO_3 or not (see “Discussion” section). Thus, the overall growth rates of calcifiers decrease more steeply with decreasing temperature than those of non-calcifiers. Second, somatic growth of calcifiers should always be slower than that of non-calcifiers, when temperature and other conditions are equal (see “Discussion” section). This is a principle deductively reached from the optimal allocation theory assuming the energetic tradeoff between somatic and exoskeletal growth (Irie and Iwasa 2005; Irie et al. 2010). Consequently, the

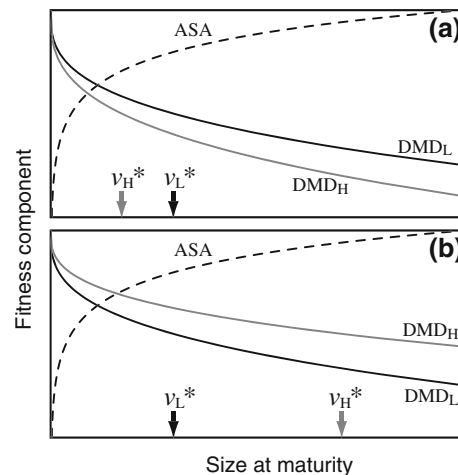


Fig. 1 The relationship between temperature and the optimal size at maturity depends on growth rates. For simplicity, we refer to the model assuming a positive relationship between temperature and mortality as indicating an adaptive significance of the TSR. The optimal size at maturity, defined as the size maximizing fitness, is determined by the balance between the adult size advantage (ASA) and the delayed maturation advantage (DMD). The black (v_L^*) and gray (v_H^*) downward arrows indicate the optimal sizes at maturity at lower and higher temperatures, respectively. The ASA curve does not depend on temperature in this case (see “Appendix 1”). **a** Lower temperatures lead to larger optimal size at maturity when the negative impact of low temperature on growth rates is relatively small (i.e., the TSR is adaptive). **b** The TSR-type reaction norm is selected against when the growth significantly slows down by low temperature

costs may outweigh the benefits of achieving a large adult body size in calcifying ectotherms, resulting in smaller rather than larger size at lower temperatures. Although being straight forward, this hypothesis has not been tested thus far. Note here that most studies on the TSR have focused on (non-calcifying) terrestrial organisms (Partridge and French 1996; Nylín and Gotthard 1998; Karl et al. 2008), while studies on calcifying marine organisms are exceedingly rare (but see O’Dea and Okamura 2000; Hosono 2011).

Against the above background, we here test experimentally whether the gold-ringed cowry, *Monetaria annulus* (Linnaeus 1758), being a marine intertidal gastropod, follows the TSR and thereby whether the costs associated with calcification may break the TSR. An alternative hypothesis is that such costs are minimal across the thermal range that we employ, and thus, the TSR-type reaction norm appears.

Materials and methods

Study organism

Monetaria annulus is an intertidal gastropod that comprises a well-suited model for studying the TSR and thermal

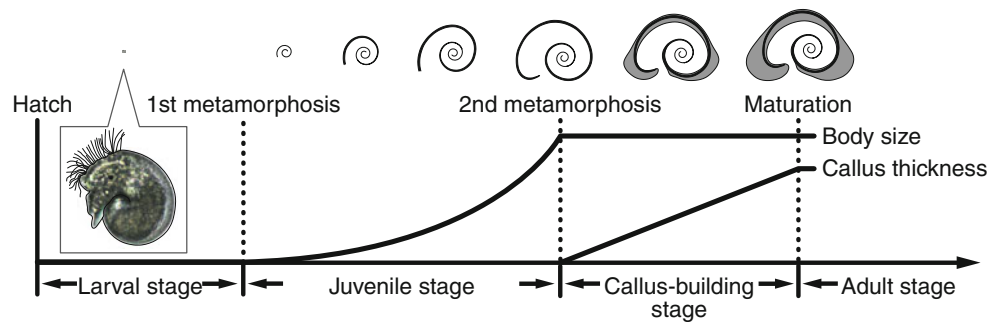


Fig. 2 Overview of the ontogeny of the marine gastropod *Monetaria annulus*. Shown are the different developmental stages, schematic anterior cross-sections of the shell, and the increases in body size and shell thickness throughout ontogeny. Ontogeny begins with a pelagic larval stage, in which the veliger larvae have a minute conical shell, termed “veliconch.” After settling on the bottom of the sea (first metamorphosis), juveniles secrete a new shell whorl on their veliconch. During the juvenile stage, they continue to expand the

juvenile shell and increase in body mass (=indicated by a solid line) until the second metamorphosis, at which shell aperture narrows and body size is fixed. In the subsequent “callus-building” stage, the thickness of the external callus (=indicated by a solid line) increases by coating the outer surface of the juvenile shell with calcareous material. Eventually shell construction stops, after which individuals reach sexual maturity and reproduction begins

adaptation in general, because this species occurs in a wide range of thermal environments. It has a wide latitudinal distribution throughout the Indo-Pacific tropics and subtropics and is found in different types of habitat, for example, in small tide pools with intense heat stress and in subtidal habitats without thermal stress (Katoh 1989; Irie 2006).

Ontogeny after the planktonic stage consists of the juvenile, the callus-building, and the reproductive stage (Fig. 2). Somatic growth and shell construction take place during the juvenile stage, which starts with a metamorphosis from planktotrophic to benthic lifestyle through settlement and ends with the second metamorphosis at which body size is fixed. All cowries exhibit explicit determinate growth (sensu Kozłowski and Wiegert 1987), because no somatic growth occurs after the juvenile stage. The callus is considered to be built for physical defense against predators (Irie and Iwasa 2003, 2005). Both juvenile shell and callus are purely composed of aragonite (T. Irie, unpublished data). In the present study, we focus on the shell size at the end of the juvenile stage (hereinafter referred to as “size at metamorphosis”), which is a good proxy of soft body size at metamorphosis (Irie and Adams 2007).

Experimental design

We performed three experiments with two constant rearing temperatures each to investigate the effects of developmental temperature on body size in *M. annulus* (Table 1). Since rearing planktonic larvae is not feasible, we collected juvenile *M. annulus* from a wild population at the Sesoko coast (see Irie 2006; Irie and Morimoto 2008) during low tides in early winter for each experiment (see Table 1 for sample sizes). Juveniles were immediately transferred to Sesoko Station (Tropical Biosphere Research Center,

University of the Ryukyus). Initial shell width (IW; Fig. 3) was measured for incorporating into the statistical model in order to control the effect of growth prior to collection (see “Statistical analyses” below). All juveniles were placed individually into 500-ml plastic bottles supplied with fresh seawater and randomly divided among two temperature-controlled water tanks with a higher or a lower temperature.

In the three experiments, different temperatures were used (cf. Table 1) as (1) no a priori information about minimum and maximum temperatures for juvenile development were available and (2) to test for the effects of different amplitudes on body size. In experiment 1, 21 and 27 °C were used, corresponding to the average ambient temperatures in the coldest and warmest months, respectively, at the field sampling site (see Irie and Fischer 2009). In experiment 2, cowries were reared at 30 and 33 °C for examining patterns in a higher temperature range. In experiment 3, finally, 24 and 34 °C were used, corresponding to maximum temperature per hour in the coldest and warmest month, respectively. We could not use more than two treatments at once because (1) the number of juveniles collected at a time, (2) the amount of algae cultured for ad libitum food supply, and (3) the electric supply to maintain the temperature of running seawater were limited. Temperatures within bottles were recorded hourly by digital data loggers (Thermochron: DS1921G-F50), showing only slight deviations from the preset temperatures (Table 1). Nevertheless, rearing temperatures fluctuated slightly throughout the experiments in response to the thermal fluctuation of incoming seawater (Table 1). Cowries were provided with algae for feeding ad libitum throughout all experiments. See Irie and Morimoto (2008) for detailed information on rearing equipment, daily maintenance, and algae cultures.

Table 1 Thermal conditions, sample sizes and timing of experiments 1–3

Thermal treatment	Experiment 1		Experiment 2		Experiment 3	
	Lower	Higher	Lower	Higher	Lower	Higher
Mean (°C)	21.35	27.04	30.41	32.81	24.04	34.07
SD (°C)	0.35	0.32	0.40	0.45	0.61	0.53
Number of females	15	21	22	17	32	28
Number of males	16	13	15	18	13	18
Starting date	Nov. 26, 2007		Dec. 14, 2008		Nov. 19, 2009	

Each experiment included a higher and lower temperature treatment. Given are the arithmetic means and sample standard deviations of hourly temperature measurements and the starting data per treatment and experiment

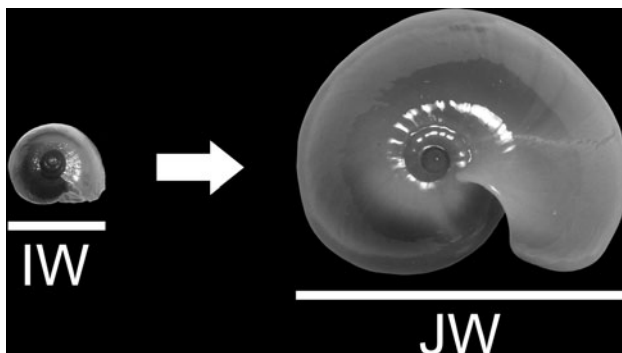


Fig. 3 Exemplary anterior views of juveniles at the beginning of the experiments (left) and at the second metamorphosis (right). *IW* and *JW* indicate the initial shell width and the juvenile shell width at metamorphosis, respectively

At the end of the juvenile stage, cowries dome the final shell whorl upwards and eventually narrow the shell aperture by turning the outer lip inwards. We defined the final day of the juvenile stage (=day of metamorphosis) by the construction of the final outer lip and measured the juvenile shell width at this time (*JW*; Fig. 3) as size at metamorphosis. Additionally, we measured development time as days to metamorphosis (*DTM*), that is, from the onset of the rearing experiment until metamorphosis. Following metamorphosis, the external shells of all individuals were broken to determine the sex anatomically, because living cowries cannot be sexed.

Statistical analyses on metamorphic size

To test the null hypothesis that the size at metamorphosis is not significantly different among temperature treatments, metamorphic size (*JW*) was analyzed by applying an ANCOVA model with experimental year, temperature, and sex as fixed-effect factors and *IW* as a covariate. To

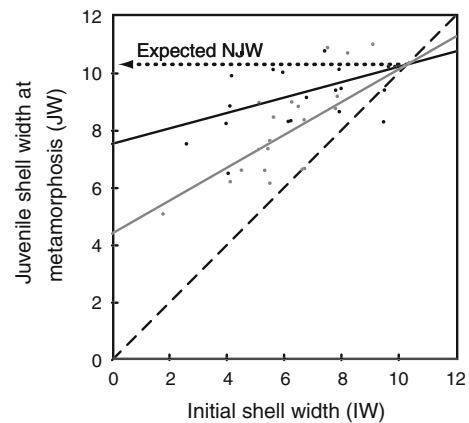


Fig. 4 Simulated data on the size at metamorphosis for individuals (with different initial size) reared at lower and higher temperatures, used here for illustrative purposes. *Solid lines* are regression lines calculated from juvenile shell width at metamorphosis (*JW*) plotted against initial shell width (*IW*), as measured in reared individuals (*dots*). Each regression line has a unique slope and y-intercept (designated as *a* and *b* in the main text, respectively). *Black* and *gray dots* indicate the data from the lower and the higher temperature treatment, respectively. The native size at metamorphosis (*NJW*) is the expected shell width at metamorphosis for individuals staying in the wild until metamorphosis (see also “Appendix 2”). Since *IW* and *JW* are equal for $Y = X$ (*dashed line*), the intersection point of *solid* and *dashed lines* indicates the expected *NJW*. Note that the two *solid lines* are expected to intersect on the *dashed line*, because the individuals who stayed in the wild were not subject to any differential experimental treatments

improve the estimation, we incorporated the assumption into the model that the expected *JW* of the individuals staying in the wild until metamorphosis is identical between the two treatments (see “Appendix 2”; Irie and Morimoto 2008). In this case, the null hypothesis to be tested is that the slopes of the regression lines of *JW* on *IW* are identical between the two thermal treatments (i.e., $a_L = a_H$; see Fig. 4 and “Appendix 2”). Thus, rejecting the null hypothesis is a necessary condition to demonstrate that *M. annulus* follows the TSR. The null hypothesis was tested using $F \equiv \frac{(RSS_{\text{null}} - RSS_{\text{alt}}) / (\theta_{\text{alt}} - \theta_{\text{null}})}{RSS_{\text{alt}} / (n - \theta_{\text{alt}})}$, where θ is the number of parameters to be estimated and n is the total number of individuals with available data. The subscript “null” indicates the null model, in which no constraint was imposed on the parameter values of y-intercept (*b*), but the slope (*a*) must be identical between the two temperatures (i.e., $a_L = a_H$; see Fig. 4 and “Appendix 2”). On the other hand, all the parameters are free in the alternative model, abbreviated with “alt” (see Faraway 2002; Ruppert et al. 2003). Assuming that the residuals in the full model follow a normal distribution, the statistic has an *F*-distribution with $\theta_{\text{alt}} - \theta_{\text{null}}$ and $n - \theta_{\text{alt}}$ degrees of freedom. Please refer to the discussion for a justification of the statistical approach used here.

In addition to the above parametric tests, we used a bootstrap approach because sample sizes in our experiments were relatively low and the mathematical assumptions on residual distributions may not be fully met. Therefore, the F -value calculated from the original data was compared with a bootstrap distribution constructed by repeating the following steps 10,000 times: (1) randomly resample the data with replacement across the two thermal treatments, keeping the sample size of each sex equal to the original one; (2) calculate F for the newly generated data after fitting regression lines. We rejected the null hypothesis at the 5 % level of significance, that is, when the original F -value was in the top 5 % of the bootstrap distribution (Efron and Tibshirani 1993; Davison and Hinkley 1997).

Statistical analyses on growth period

Larger maturation size is often accompanied by a prolonged growth period at lower temperatures. In our experiments, individuals with a small initial size needed longer until metamorphosis, particularly when reared at low temperatures. Consequently, the dispersion of DTM potentially depends on both initial shell size and rearing temperature. We thus assumed that the DTM follows a lognormal distribution, in which the mean and the variance are positively interdependent, in order to test the null hypothesis that the median is identical between the two different temperature regimes.

The null hypothesis that the median DTM is identical between the two rearing temperatures was tested by calculating the likelihood ratio test statistic, given as $D = -2\ln(L_{\text{null}}/L_{\text{alt}}) = -2(LL_{\text{null}} - LL_{\text{alt}})$, where L and LL are the maximum likelihood and its logarithm, respectively (see “Appendix 3”). The subscript “null” indicates the null model, in which no constraint was imposed on the parameter values of the scale parameter (σ^2), but the location parameters (α and β) must be identical between the two temperatures (i.e., $\alpha_L = \alpha_H$ and $\beta_L = \beta_H$). On the other hand, all the parameters are free in the alternative model, abbreviated with “alt.” The statistic D approximately follows a χ^2 -distribution with the degree of freedom being equal to the difference in the number of free parameters between the null and alternative model.

Since the χ^2 -approximation may not be sufficiently reliable, we performed again bootstrap tests by comparing the D -value calculated from the original data with a bootstrap distribution constructed by repeating the following steps 10,000 times: (1) randomly resample the data with replacement across the two thermal treatments, keeping the sample size of each sex equal to the original one; (2) calculate D for the newly generated data after

fitting the above model. We rejected the null hypothesis at the 5 % level of significance, that is, when the original D -value was in the top 5 % of the bootstrap distribution (Efron and Tibshirani 1993; Davison and Hinkley 1997).

Results

In agreement with the TSR, *M. annulus* exhibited a remarkable trend toward smaller size at metamorphosis when reared at higher developmental temperatures, particularly so in females (Fig. 5). When pooling across experiments and sexes, this pattern was statistically significant regardless of whether the F -approximation or bootstrapping method was used (Table 2). When analyzing experiments separately though, differences between rearing temperatures were only significant in experiment 3, in which the temperature difference was largest (Table 2). Likewise, when pooling across experiments significant differences were restricted to females, while for males only a trend was detected. The good agreement between F -approximation and bootstrapping (Table 2) is consistent with the residual normality in our data, as tested with a Shapiro–Wilk test ($W = 0.993$, $n = 228$, $P > 0.05$).

Given equal initial shell size, *M. annulus* had a longer growing period at lower than at higher temperatures, except in experiment 2 (Fig. 6; Table 3). This pattern was statistically significant throughout, except for experiment 2 in which the temperature difference was relatively small (Table 3; Fig. 6c, d). Results of χ^2 -approximation versus bootstrapping generally yielded very similar results (Table 3).

Discussion

In the present experiments, *M. annulus* reared at lower temperatures matured at a larger size and had a longer growing period, at least if the thermal difference between the two treatments was sufficiently large. These results suggest that this species does follow the TSR. The notion that *M. annulus* thus does not comprise an exception from the TSR is consistent with field data, showing that individuals developing in warmer seasons metamorphose at a smaller size than those that grow in cooler seasons (Irie and Fischer 2009). Especially, the results obtained from experiment 3 (10 °C difference) are in good agreement with these field data (Irie and Fischer 2009).

We had assumed in our working hypothesis that lower temperatures entail more energy to precipitate a certain amount of CaCO_3 . To verify this assumption, the saturation

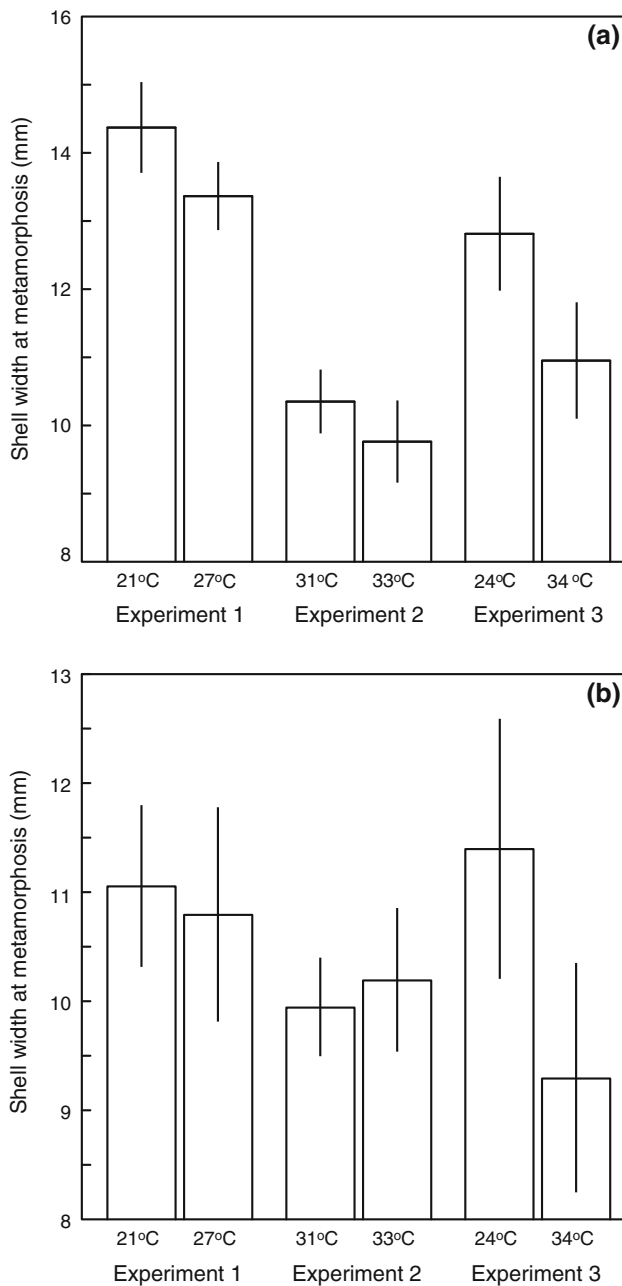


Fig. 5 Estimated size at metamorphosis (JW) at IW = 0 for (a) females and (b) males. This value corresponds to the y-intercept (b) of the regression line of JW on IW (see Fig. 4 and “Appendix 2”). Error bars indicate the bootstrap standard errors

state of seawater with respect to aragonite, $\Omega_{ar} = [\text{Ca}^{2+}][\text{CO}_3^{2-}]/K_{sp}$, where $[\text{Ca}^{2+}]$ and $[\text{CO}_3^{2-}]$ are the concentrations of calcium and carbonate ions, respectively, needs to be considered. The solubility product, K_{sp} , increases with decreasing temperature, which is the reason why aragonite becomes more soluble at lower temperatures (e.g., Plummer and Busenberg 1982; Vermeij 1987). Theoretically, aragonite precipitates from seawater when $\Omega_{ar} > 1$ and dissolution occurs when $\Omega_{ar} < 1$ (e.g., Peterson 2010). In fact, there can be no doubt that the surface

Table 2 Statistical results for the effects of rearing temperature on shell width at metamorphosis (JW)

	All data	1st year	2nd year	3rd year	Female	Male
n	228	65	72	91	135	93
θ_{alt}	18	6	6	6	9	9
RSS_{alt}	206.562	45.779	36.590	124.192	119.985	86.580
θ_{null}	12	4	4	4	6	6
RSS_{null}	224.165	47.507	37.666	138.992	130.113	94.054
F	2.983	1.113	0.971	5.065	3.545	2.417
p_{approx}	0.008	0.335	0.384	0.008	0.017	0.072
p_{boot}	0.007	0.359	0.387	0.006	0.010	0.069

n , sample size; θ , the number of estimated parameters; RSS , the residual sum of squares; F , F -value calculated from the data; p_{approx} , the p value based on the F -approximation; p_{boot} , the p value based on the bootstrapping method. Subscripts “alt” and “null” refer to the alternative and the null model, respectively. Significant p values are given in bold

seawater in Okinawa is oversaturated with respect to aragonite ($\Omega_{ar} > 3$ throughout the year; for example, Ishii et al. 2011; Feely et al. 2012) and so it is in our experiments (i.e., 21–34 °C). Thus, calcification may actually incur very little costs challenging our original hypothesis. However, marine calcifiers are known to keep the Ω_{ar} at the place of calcification much higher than 1. For example, the golfball coral, *Favia fragum*, maintains the calcifying fluid Ω_{ar} at around 15, when the Ω_{ar} of external seawater is ~ 2.4 (Cohen et al. 2009; Cohen and Holcomb 2009). In addition, the speed of calcification increases with increasing external Ω_{ar} even when $\Omega_{ar} > 1$ (Marubini and Atkinson 1999; Ohde and Hossain 2004). Marine calcifiers thus seem to pay an energetic cost to elevate the Ω_{ar} in the calcifying fluid by decreasing pH and increasing the calcium ion concentration by a $\text{Ca}^{2+}/\text{H}^{+}$ exchanger (Ca^{2+} -ATPase) across the mantle membrane (Cohen and McConnaughey 2003; McConnaughey and Gillikin 2008). This is probably needed because $\Omega_{ar} > 1$ is not sufficient for the precipitation of aragonite (see Cohen and Holcomb 2009). In summary, lower temperatures entail more energy to maintain a constant level of the calcifying fluid Ω_{ar} , because Ω_{ar} decreases with decreasing temperature. This is the rational behind the idea that the overall growth rates of calcifiers decrease more steeply with decreasing temperature than those of non-calcifiers (see “Appendix 1”).

Our working hypothesis also assumes that the very slow growth due to calcification at low temperatures may withdraw any adaptive advantage of the TSR, such that reaction norms converse to the TSR may have evolved in calcifying ectotherms (see “Appendix 1”). Molluscan shells are composed of inorganic crystal (CaCO_3) and an organic matrix within and between crystals, both of which require energetic costs to produce (Palmer 1983, 1992).

Fig. 6 Median regression curves calculated from days to metamorphosis (DTM) plotted against initial shell width (IW) for individuals reared at a lower (black dots) or a higher temperature (gray dots). **a** Females, first experiment. **b** Males, first experiment. **c** Females, second experiment. **d** Males, second experiment. **e** Females, third experiment. **f** Males, third experiment

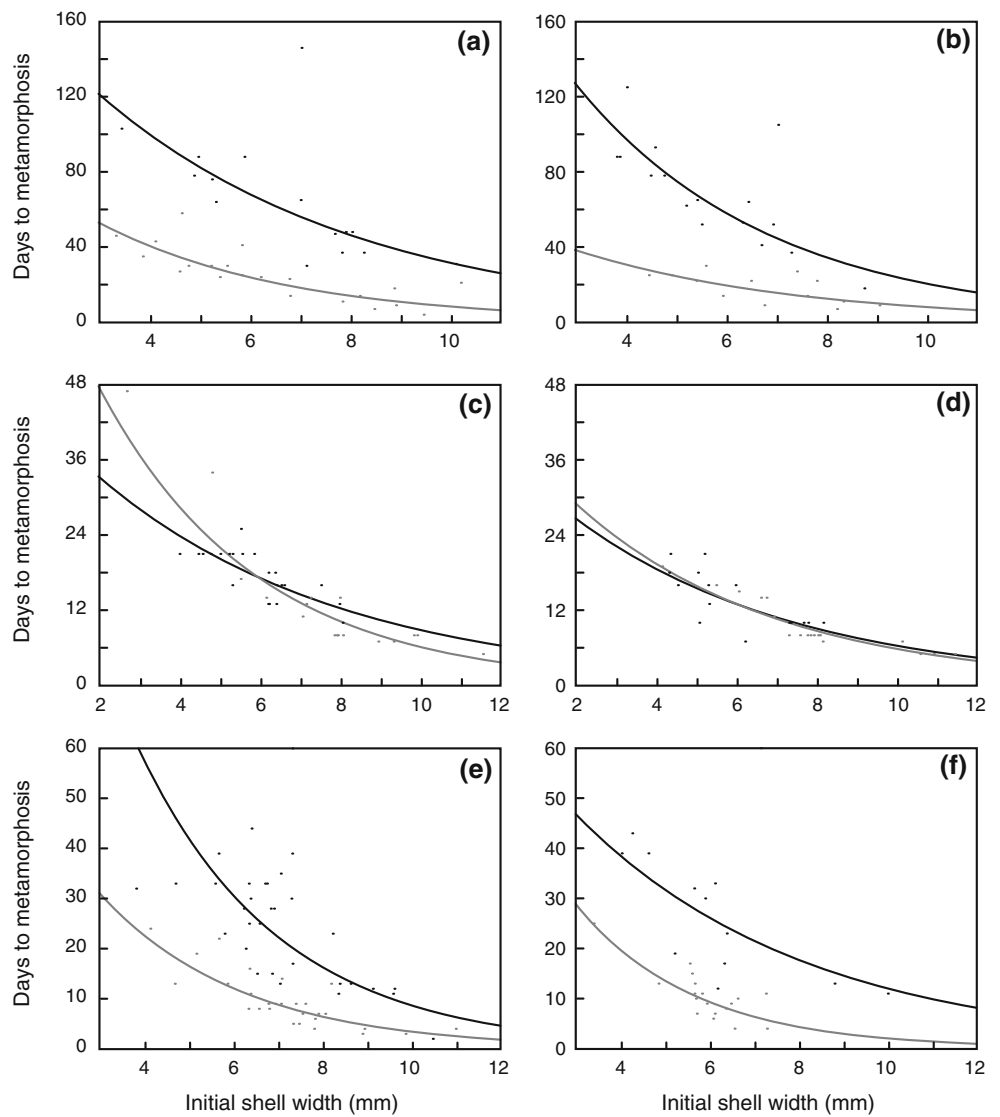


Table 3 Statistical results for the effects of rearing temperature on days to metamorphosis (DTM)

	All data	1st year	2nd year	3rd year	Female	Male
<i>n</i>	228	65	72	91	135	93
θ_{alt}	36	12	12	12	18	18
LL_{alt}	-686.563	-249.723	-157.942	-278.898	-415.112	-271.451
θ_{null}	24	8	8	8	12	12
LL_{null}	-774.556	-289.154	-161.069	-324.332	-467.374	-307.181
<i>D</i>	175.986	78.864	6.254	90.868	104.525	71.462
p_{approx}	<10⁻³⁰	<10⁻¹⁵	0.181	<10⁻¹⁸	<10⁻¹⁹	<10⁻¹²
p_{boot}	<10⁻⁴	<10⁻⁴	0.260	<10⁻⁴	<10⁻⁴	<10⁻⁴

n, sample size; θ , the number of estimated parameters; *LL*, log-likelihood; *D*, *D*-value calculated from the data; p_{approx} , the *p* value based on the χ^2 -approximation; p_{boot} , the *p* value based on the bootstrapping method. Subscripts “alt” and “null” refer to the alternative and the null model, respectively. Significant *p* values are given in bold

Including the cost of synthesizing the organic component, the total energy to construct shells seems to be quantitatively comparable to that of somatic growth (e.g., Palmer

1992). Accordingly, there is an energetic tradeoff between somatic and skeletal growth (Irie and Iwasa 2005; Irie et al. 2010). This suggests that calcifying ectotherms always

grow more slowly than shell-less ones, if energy income and other conditions are equal (but see Bourdeau 2010, proposing a tradeoff-free mechanism that makes thicker shells induced by slower somatic growth due to lower food availability). Furthermore, shell building may limit the rate of somatic growth if low temperatures retard shell building more strongly than somatic growth, because body growth cannot proceed in advance of skeletal growth (Palmer 1981).

Nevertheless, our data do not support the above expectation. An explanation is that the fitness loss due to shell building at low temperatures was not high enough to break the TSR in *M. annulus*. In other words, the energetic cost of shell building might be too low. On the other hand, low temperatures substantially extended the juvenile stage in our experiments. In experiment 1, for example, the growth period at 21 °C was more than twice as long as at 27 °C, while mean maturation size was nearly the same between the two treatments. Hence, a prolonged growth period may compensate the very slow growth at low temperatures in order to avoid reduced adult size.

Another possible explanation for our results is that there is some fundamental constraint resulting in the TSR. This idea was supported by the finding that larger body size at lower temperature is caused by an increase in cell size, while the number of cells remained constant in *Caenorhabditis elegans* (van Voorhies 1996). This hypothesis implicitly assumes that the negative relationship between temperature and cell size is invariable due to a genetic or physiological constraint, suggesting that the TSR itself has no adaptive significance. However, this hypothesis was rejected by Kammenga et al. (2007), who discovered a wild-type strain of *C. elegans* not following the TSR. Even if such a constraint would exist, natural selection should be able to break the TSR by working on the slope of the reaction norm, which is supported by the occurrence of several exceptions to the TSR at the species and population level (Atkinson 1995; Walters and Hassall 2006; Zuo et al. 2012).

Interestingly, females showed a much stronger response to different rearing temperatures than males in our experiments. This might be a consequence of the female-biased sexual size dimorphism in *M. annulus* (Irie and Adams 2007; Irie and Morimoto 2008). Thus, juvenile males are more developed than females at the start of rearing when initial size is equal between the sexes. Therefore, males may have been exposed to controlled thermal conditions for a shorter period of time than females, leaving less opportunity to respond to a temperature change. Alternatively, the costs and benefits associated with plastic responses to temperature may differ across the sexes (e.g., in butterflies; see Fischer and Fiedler 2000, 2001).

In summary, our results suggest that *M. annulus* does conform to the TSR. The associated plastic response to

differences in the developmental environment may also affect macrogeographic patterns of adult body size in cowries. Tissot (1984) demonstrated that the congener *M. caputserpentis* exhibits a latitudinal size cline from southeast Africa to the west Pacific, by showing that shell size at metamorphosis correlates negatively with average seawater temperature (see also Irie 1997; Irie and Iwasa 2003). Similar trends were found in other cypraeid species, for example, *Cypraea tigris* (Kay 1961; Foin 1972), *Mauritia arabica* (Schilder 1961), and *Erronea erronea* (Schilder and Schilder 1968). It is currently unknown whether such clines result from genetic adaptation or phenotypic plasticity (Tissot 1984, 1988; Irie 1997, 2006; Irie and Iwasa 2003), but our current results suggest that the latter possibility should not be dismissed.

Acknowledgments The authors are grateful to P. Kraufvelin, W. C. E. P. Verberk, W. Zuo, and three anonymous reviewers for valuable comments, and to S. Nakamura and Y. Nakano for maintaining the equipment necessary for rearing experiments at Sesoko Station. We also thank K. Baba, Y. Iwasa, K. Sakai, S. Tuljapurkar, and K. Yamahira for helpful discussions. This project was funded by the Japan Society for the Promotion of Science (JSPS).

Appendix 1: Mathematical proof for the working hypothesis

Assuming that the instantaneous mortality rate, μ , is independent of age or size, the lifetime reproductive success (R_0) of a determinate grower is simply given by

$$R_0 = M_x \times L_x \times \int_0^{\infty} e^{-\mu t} dt \quad (1)$$

where M_x is the age-independent fecundity rate of an individual that matures at age x , L_x is the probability that the individual survives until maturity (i.e., $L_x = e^{-\mu x}$), and t is the age after maturity (i.e., $t = -x$ at birth). Taking the natural logarithm of R_0 leads to

$$\ln R_0 = \ln M_x + \ln L_x - \ln \mu, \quad (2)$$

where the first term on the right-hand side can be regarded as the adult size advantage (ASA), if fecundity increases with increasing size. On the other hand, the second term is the delayed maturation disadvantage (DMD), because a longer growth period decreases the survivorship until maturity. Let $v(a, x)$ be the size at maturity of an individual that matures at age x with growth rates, a , where growth rates (a) is passively and uniquely determined by temperature, θ . If x^* and v^* designate the age and size at maturity that maximize the fitness R_0 , then the dependency of the optimal size at maturity (v^*) on temperature (θ) is

$$\frac{dv^*}{d\theta} = \frac{\partial v^*}{\partial a} \frac{\partial a}{\partial \theta} + \frac{\partial v^*}{\partial \mu} \frac{\partial \mu}{\partial \theta}, \tag{3}$$

where $\partial\mu/\partial\theta > 0$ is assumed to reflect adaptive significance of the TSR.

To illustrate the above results, we assign specific functions to the growth and fecundity functions: $dv/dx = av^k$ and $M_x = v(x)^k$, respectively. k is a coefficient for metabolism that often takes a value of two-thirds. Approximating the initial size $v(0)$ to zero, maturation size is explicitly given as $v(x) = (a(1 - k)x)^{1/(1-k)}$. From Eq. (2), $ASA = k \ln v(x)$ and $DMD = -\mu x = -\mu v(x)^{1-k}/a(1 - k)$ in this case (see Fig. 1). Taking the derivative of $\ln R_0$ with respect to x , equation it to zero, and solving it for x gives the optimal age at maturity, $x^* = k/(1 - k)\mu$, and thus $v^* = v(x^*) = (ak/\mu)^{1/(1-k)}$. The necessary condition that the TSR is selected against is

$$\frac{\partial v^*}{\partial a} \frac{\partial a}{\partial \theta} > -\frac{\partial v^*}{\partial \mu} \frac{\partial \mu}{\partial \theta}, \tag{4}$$

which is obtained by setting the right-hand side of Eq. (3) to be positive and then rearranging it. When $dv/dx = av^k$ and $M_x = v(x)^k$, we have

$$\frac{1}{a} \frac{\partial a}{\partial \theta} > \frac{1}{\mu} \frac{\partial \mu}{\partial \theta}, \tag{5}$$

or equivalently,

$$\frac{\partial \ln a}{\partial \theta} > \frac{\partial \ln \mu}{\partial \theta}. \tag{6}$$

This inequality suggests that the TSR is more likely to be broken when (1) growth rates (a) are small, (2) growth rates (a) decrease more steeply with temperature (θ), or (3) both. The same conclusion is reached when assuming the linear growth function [i.e., $v(x) = ax$], for example.

Appendix 2: Incorporating NJW into the ANCOVA model

Prior to the statistical analyses on metamorphic size, we defined the “native shell width at metamorphosis” (NJW) as the shell width at metamorphosis of the individuals staying in the wild until metamorphosis (Fig. 4; see also Irie and Morimoto 2008). The NJW should be identical between the two treatments, because the individuals who stayed in the wild until metamorphosis were subject to the common environmental conditions. We incorporated this into our statistical model in order to improve the estimation of regression lines. NJW can be estimated as the intersection point between the regression line of JW on IW and the diagonal line (Fig. 4). As the individuals with the same sex and from the same experiment have the same expected

NJW, the regression coefficients, a and b , can be estimated by minimizing the total sum of residual squares, $RSS = \phi_F + \phi_M$. The sum of residual squares for females (ϕ_F) and males (ϕ_M) are given as

$$\begin{aligned} \phi_F = & \sum_{i=1}^{N_{FL}} \{JW_i - (a_{FL}IW_i + b_{FL})\}^2 \\ & + \sum_{i=1}^{N_{FH}} \{JW_i - (a_{FH}IW_i + b_{FH})\}^2 \end{aligned} \tag{7}$$

and

$$\begin{aligned} \phi_M = & \sum_{i=1}^{N_{ML}} \{JW_i - (a_{ML}IW_i + b_{ML})\}^2 \\ & + \sum_{i=1}^{N_{MH}} \{JW_i - (a_{MH}IW_i + b_{MH})\}^2, \end{aligned} \tag{8}$$

where IW_i and JW_i are initial shell width and juvenile shell width at metamorphosis, respectively, for i -th individual out of N total individuals. Subscripts F and M signify females and males, respectively. Similarly, subscripts L and H denote the lower and the higher temperature treatments conducted in the same year, respectively. Using the least-square estimates of the regression slope (\hat{a}) and the y-intercept (\hat{b}), the expected NJW is calculated as:

$$E[NJW] = (1 - \hat{a})/\hat{b}. \tag{9}$$

Since the expected NJW is identical between the two temperature treatments (but not between the sexes) within one experiment, it follows that:

$$\frac{1 - \hat{a}_L}{\hat{b}_L} = \frac{1 - \hat{a}_H}{\hat{b}_H}, \tag{10}$$

which reduces the number of parameters to be estimated. All the least-square estimates were numerically computed using Mathematica (version 7 for Windows, Wolfram Research, Champaign, IL).

One may argue that our data could be equally well analyzed by applying an ordinary ANCOVA method with JW as the dependent variable, IW as the covariate, and temperature and sex as fixed-effect factors. In this case, the interaction effect between IW and temperature should be significant if sample size is sufficiently large; then the conformance to the TSR is accepted when a higher rearing temperature leads to smaller y-intercept (see Fig. 4). However, regression lines were sometimes unstable (i.e., slopes were too steep to attain a meaningful interpretation) in our data, probably because our sample sizes were relatively low and IW was not scattered broadly enough. This is the main reason why we implemented a model with a mathematical constraint designated by Eq. (10), instead of performing an ordinary ANCOVA. Except for this point,

our method is mathematically equivalent with ANCOVA, which should be noticed by looking at using the least-square regression lines and the F -statistic computed by dividing the explained variance between groups by the unexplained variance within the groups.

Appendix 3: ML estimation of the lognormal regression parameters

If $Y (>0)$ is a random variable that follows a lognormal distribution and linearly depends on a positive covariate, x , its probability density function is expressed as:

$$g(y|x; \alpha, \beta, \sigma^2) = \frac{1}{y\sqrt{2\pi\sigma^2}} \exp\left[-\frac{(\ln y - (\alpha + \beta x))^2}{2\sigma^2}\right], \quad (11)$$

where the parameters are $\alpha \in \mathfrak{R}$, $\beta \in \mathfrak{R}$, and $\sigma^2 > 0$. In this case, the median of Y is given as $\text{Med}[Y] = \exp[\alpha + \beta x]$. The maximum likelihood estimates of the parameters are those that maximize the likelihood function:

$$L(\alpha, \beta, \sigma^2) = \prod_{i=1}^n \frac{1}{y_i \sqrt{2\pi\sigma^2}} \exp\left[-\frac{(\ln y_i - (\alpha + \beta x_i))^2}{2\sigma^2}\right], \quad (12)$$

or its logarithmic form:

$$LL(\alpha, \beta, \sigma^2) = -\frac{n}{2} \ln(2\pi\sigma^2) - \sum_{i=1}^n \ln y_i - \frac{1}{2\sigma^2} \sum_{i=1}^n (\ln y_i - (\alpha + \beta x_i))^2, \quad (13)$$

where y_i is DTM and x_i is IW for the i -th individual out of n individuals. Taking the partial derivative of LL with respect to each parameter and equating it to zero yields:

$$\hat{\alpha} = \frac{1}{n} \left(\sum_{i=1}^n \ln y_i - \hat{\beta} \sum_{i=1}^n x_i \right), \quad (14a)$$

$$\hat{\beta} = \left(\sum_{i=1}^n x_i \ln y_i - \hat{\alpha} \sum_{i=1}^n x_i \right) / \sum_{i=1}^n x_i^2, \quad (14b)$$

and

$$\hat{\sigma}^2 = \frac{1}{n} \sum_{i=1}^n \left\{ \ln y_i - (\hat{\alpha} + \hat{\beta} x_i) \right\}^2, \quad (14c)$$

respectively (the “hat” indicates the maximum likelihood estimate of each parameter). Simultaneous Eqs. (14a) and (14b) provide an explicit function of $\hat{\alpha}$:

$$\hat{\alpha} = \frac{\sum_{i=1}^n x_i^2 \sum \ln y_i - \sum x_i \sum x_i \ln y_i}{n \sum x_i^2 - (\sum x_i)^2}, \quad (15)$$

which also gives the maximum likelihood estimates of β and σ^2 from Eqs. (14b) and (14c).

References

- Angilletta MJ, Dunham AE (2003) The temperature-size rule in ectotherms: simple evolutionary explanations may not be general. *Am Nat* 162:332–342
- Angilletta MJ, Steury TD, Sears MW (2004) Temperature, growth rate, and body size in ectotherms: fitting pieces of a life-history puzzle. *Integr Comp Biol* 44:498–509
- Arendt JD (2010) Size-fecundity relationships, growth trajectories, and the temperature-size rule for ectotherms. *Evolution* 65:43–51
- Atkinson D (1994) Temperature and organism size—a biological law for ectotherms? *Adv Ecol Res* 25:1–58
- Atkinson D (1995) Effects of temperature on the size of aquatic ectotherms: exceptions to the general rule. *J Therm Biol* 20:61–74
- Atkinson D (1996) Ectotherm life-history responses to developmental temperature. In: Johnston IA, Bennett AF (eds) *Animals and temperature: phenotypic and evolutionary adaptation*. Cambridge University Press, Cambridge, pp 61–74
- Atkinson D, Ciotti BJ, Montagnes DJS (2003) Protists decrease in size linearly with temperature: ca. 2.5% °C⁻¹. *Proc R Soc Lond B* 270:2605–2611
- Bourdeau PE (2010) An inducible morphological defence is a passive by-product of behaviour in a marine snail. *Proc R Soc B* 277:455–462
- Cohen AL, Holcomb M (2009) Why corals care about ocean acidification: uncovering the mechanism. *Oceanography* 22:117–127
- Cohen AL, McConnaughey TA (2003) Geochemical perspectives on coral mineralization. In: Dove PM, Weiner S, deYoreo JJ (eds) *Biomaterialization. Reviews in mineralogy and geochemistry* 54. The Mineralogical Society of America, Washington DC, pp 151–187
- Cohen AL, McCorkle DC, de Putron S, Gaetani GA, Rose KA (2009) Morphological and compositional changes in the skeletons of new coral recruits reared in acidified seawater: Insights into the biomineralization response to ocean acidification. *Geochem Geophys Geosystems*, 10:Q07005
- Davison AC, Hinkley DV (1997) *Bootstrap methods and their applications*. Cambridge University Press, Cambridge
- Efron B, Tibshirani RJ (1993) *An introduction to the bootstrap*. Chapman & Hall/CRC, New York
- Faraway JJ (2002) *Practical regression and anova using R*. <http://www.maths.bath.ac.uk/~jjf23/book/>
- Feely RA, Sabine CL, Byrne RH, Millero FJ, Dickson AG, Wanninkhof R, Murata A, Miller LA, Greeley D (2012) Decadal changes in the aragonite and calcite saturation state of the Pacific Ocean. *Global Biogeochem Cycles* 26:GB3001
- Fischer K, Fiedler K (2000) Sex-related differences in reaction norms in the butterfly *Lycaena tityrus* (Lepidoptera: Lycaenidae). *Oikos* 90:372–380
- Fischer K, Fiedler K (2001) Dimorphic growth patterns and sex-specific reaction norms in the butterfly *Lycaena hippothoe sumadiensis*. *J Evol Biol* 14:210–218
- Fischer K, Fiedler K (2002) Reaction norms for age and size at maturity in response to temperature: a test of the compound interest hypothesis. *Evol Ecol* 16:333–349
- Foin TC (1972) Ecological influences on the size of *Cypraea tigris* L., 1758, in the Pacific. *Proc Malacol Soc Lond* 40:211–218

- Hosono T (2011) Effect of temperature on growth and maturation pattern of *Caprella mutica* (Crustacea, Amphipoda): does the temperature-size rule function in caprellids? *Mar Biol* 158: 363–370
- Irie T (1997) Relationship between geographic variation of shell structure and water temperature in *Cypraea caputserpentis* (Gastropoda: Cypraeidae). *Yuriyagai* 5:17–29
- Irie T (2006) Geographic variation of shell morphology in *Cypraea annulus* (Gastropoda: Cypraeidae). *J Molluscan Stud* 72:31–38
- Irie T, Adams B (2007) Sexual dimorphism in soft body weight in adult *Monetaria annulus* (Family Cypraeidae). *Veliger* 49: 209–211
- Irie T, Fischer K (2009) Ectotherms with a calcareous exoskeleton follow the temperature-size rule—evidence from field survey. *Mar Ecol Prog Ser* 385:33–37
- Irie T, Iwasa Y (2003) Optimal growth model for the latitudinal cline of shell morphology in cowries (genus *Cypraea*). *Evol Ecol Res* 5:1133–1149
- Irie T, Iwasa Y (2005) Optimal growth pattern of defensive organs: the diversity of shell growth among mollusks. *Am Nat* 165: 238–249
- Irie T, Morimoto N (2008) Phenotypic plasticity and sexual dimorphism in size at post-juvenile metamorphosis: common-garden rearing of an intertidal gastropod with determinate growth. *Biol Bull* 215:126–134
- Irie T, Bessho K, Findlay HS, Calosi P (2010) Increasing costs due to ocean acidification drives phytoplankton to be more heavily calcified: optimal growth strategy of coccolithophores. *PLoS ONE* 5:e13436
- Ishii M, Kosugi N, Sasano D, Saito S, Midorikawa T, Inoue HY (2011) Ocean acidification off the south coast of Japan: a result from time series observations of CO₂ parameters from 1994 to 2008. *J Geophys Res* 116:C06022
- Kammenga JE, Doroszuk A, Riksen JAG, Hazendonk E, Spiridon L, Petrescu AJ, Tijsterman M, Plasterk RHA, Bakker J (2007) A *Caenorhabditis elegans* wild type defies the temperature–size rule owing to a single nucleotide polymorphism in tra-3. *PLoS Genet* 3:e34
- Karl I, Janowitz SA, Fischer K (2008) Altitudinal life-history variation and thermal adaptation in the Copper butterfly *Lycaena tityrus*. *Oikos* 117:778–788
- Katoh M (1989) Life history of the golden ring cowry *Cypraea annulus* (Mollusca: Gastropoda) on Okinawa Island, Japan. *Mar Biol* 101:227–233
- Kay A (1961) On *Cypraea tigris schilderia* Cate. *Veliger* 4:36–40
- Kingsolver JG, Huey RB (2008) Size, temperature, and fitness: three rules. *Evol Ecol Res* 10:251–268
- Kozlowski J, Wiegert RG (1987) Optimal age and size at maturity in annuals and perennials with determinate growth. *Evol Ecol* 1: 231–244
- Kozlowski J, Czarnoleski M, Danko M (2004) Can optimal resource allocation models explain why ectotherms grow larger in cold? *Integr Comp Biol* 44:480–493
- Marubini F, Atkinson MJ (1999) Effects of lowered pH and elevated nitrate on coral calcification. *Mar Ecol Prog Ser* 188:117–121
- McConnaughey TA, Gillikin DP (2008) Carbon isotopes in mollusk shell carbonates. *Geo-Mar Lett* 28:287–299
- Morse JW, Arvidson RS, Lutge A (2007) Calcium carbonate formation and dissolution. *Chem Rev* 107:342–381
- Nylin S, Gotthard K (1998) Plasticity in life-history traits. *Ann Rev Entomol* 43:63–83
- O’Dea A, Okamura B (2000) Intracolony variation in zooid size in cheilostome bryozoans as a new technique for investigating palaeoseasonality. *Palaeogeogr Palaeoclimatol Palaeoecol* 162:319–332
- Ohde S, Hossain MMM (2004) Effect of CaCO₃ (aragonite) saturation state of seawater on calcification of *Porites* coral. *Geochem J* 38:613–621
- Palmer AR (1981) Do carbonate skeletons limit the rate of body growth? *Nature* 292:150–152
- Palmer AR (1983) Relative cost of producing skeletal organic matrix versus calcification: evidence from marine gastropods. *Mar Biol* 75:287–292
- Palmer AR (1992) Calcification in marine molluscs: how costly is it? *Proc Natl Acad Sci USA* 89:1379–1382
- Partridge L, French V (1996) Thermal evolution of ectotherm body size: Why get big in the cold? In: Johnston IA, Bennett AF (eds) *Animals and temperature: phenotypic and evolutionary adaptation*. Cambridge University Press, Cambridge, pp 265–292
- Peterson LC (2010) Calcium carbonate. In: Steele JH, Thorpe SA, Turekian KK (eds) *Marine chemistry & geochemistry: a derivative of the encyclopedia of ocean sciences*, 1st edn. Academic Press, London, pp 336–345
- Plummer LN, Busenberg E (1982) The solubilities of calcite, aragonite and vaterite in CO₂-H₂O solutions between 0 and 90°C, and an evaluation of the aqueous model for the system CaCO₃-CO₂-H₂O. *Geochim Cosmochim Acta* 46:1011–1040
- Ruppert D, Wand MP, Carroll RJ (2003) *Semiparametric regression*. Cambridge University Press, Cambridge
- Schilder FA (1961) A statistical study in cowries: the size of *Mauritia arabica* (Linnaeus). *Veliger* 4:15–17
- Schilder FA, Schilder M (1968) Studies on populations of the cowrie *Erronea erronea* (Linnaeus). *Veliger* 11:109–116
- Tissot BN (1984) Multivariate analysis of geographic variation in *Cypraea caputserpentis* (Gastropoda: Cypraeidae). *Veliger* 27: 106–119
- Tissot BN (1988) Geographic variation and heterochrony in two species of cowries (genus *Cypraea*). *Evolution* 42:103–117
- van der Have TM, de Jong G (1996) Adult size in ectotherms: temperature effects on growth and differentiation. *J Theor Biol* 183:329–340
- van Voorhies WA (1996) Bergmann size clines: a simple explanation for their occurrence in ectotherms. *Evolution* 50:1259–1264
- Vermeij GJ (1987) *Evolution and escalation: an ecological history of life*. Princeton University Press, Princeton
- Walters RJ, Hassall M (2006) The temperature-size rule in ectotherms: may a general explanation exist after all? *Am Nat* 167:510–523
- Zuo W, Moses ME, West GB, Hou C, Brown JH (2012) A general model for effects of temperature on ectotherm ontogenetic growth and development. *Proc R Soc B* 279:1840–1846